SIN-like pathway kinases regulate the end of mitosis in the methylotrophic yeast *Ogataea polymorpha*

Shen Jiangyan[1], Kaoru Takegawa[1, 2], Gislene Pereira[3,4], Hiromi Maekawa[1, 2*]

1. Graduate School of Bioresources and Biotenvironmental Sciences, Kyushu University, Fukuoka, Japan
2. Faculty of Agriculture, Kyushu University, Japan
3. Centre for Organismal Studies (COS), University of Heidelberg, Germany
4. Division of Centrosomes and Cilia, German Cancer Research Centre (DKFZ), DKFZ-ZMBH Alliance, Germany

* Corresponding author
Tel: +81 92 802 4769; E-mail: hmaekawa@agr.kyushu-u.ac.jp

Running Title:
The SIN regulates mitotic exit in *O. polymorpha*

Abstract

The Mitotic exit network (MEN) is a conserved signalling pathway essential for termination of mitosis in the budding yeast *Saccharomyces cerevisiae*. All MEN components are highly conserved in the methylotrophic budding yeast *Ogataea polymorpha*, except for Cdc15 kinase. Amongst *O. polymorpha* protein kinases that have some similarity to ScCdc15, only two had no other obvious homologues in *S. cerevisiae* and these were named *OpHCD1* and *OpHCD2* for *homologue candidate of ScCdc15*. A search in other yeast species revealed that OpHcd2 has an armadillo type fold in the C-terminal region as found in SpCdc7 kinases of the fission yeast *Schizosaccharomyces pombe,* which are homologues of ScCdc15; while OpHcd1 is homologous to SpSid1 kinase, a component of the Septation Initiation Network (SIN) of *S. pombe* not present in the MEN. Since the deletion of either *OpHCD1* or *OpHCD2* resulted in lethality under standard growth conditions, conditional mutants were constructed

by introducing an ATP analog sensitive mutation. For *OpHCD2*, we constructed and used new genetic tools for *O. polymorpha* that combined the Tet promoter and the improved auxin-degron systems. Conditional mutants for *OpHCD1* and *OpHCD2* exhibited significant delay in late anaphase and defective cell separation, suggesting that both genes have roles in mitotic exit and cytokinesis. These results suggest a SIN-like signalling pathway regulates termination of mitosis in *O. polymorpha* and that the loss of Sid1/Hcd1 kinase in the MEN occurred relatively recently during the evolution of budding yeast.

(234 words)

Keywords

Mitotic Exit Network / Septation Initiation Network / *Ogataea polymorpha* / Cdc15 kinase / Auxin-dependent degradation /Tet promoter

Introduction

In eukaryotic cell division, cytokinesis is tightly linked to the completion of mitosis to ensure proper segregation of chromosomes into two daughter cells. This is particularly critical in budding yeast cell division where the site of cytokinesis (bud neck) is determined before spindle formation, so the progression of cytokinesis must be paused until nuclear division is completed and one set to chromosomes has passed through the bud neck and entered the daughter cell body. Therefore, deciding when to exit from mitosis and initiate cytokinesis is important in cell cycle regulation. In the budding yeast *Saccharomyces cerevisiae* and fission yeast *Schizosaccharomyces pombe*, the completion of mitosis is regulated by a GTPase-driven signalling pathway named Mitotic Exit Network (MEN) and Septation Initiation Network (SIN), respectively (hereafter collectively referred to as the mitotic exit (ME)-signalling pathway). The activation of MEN is essential for mitotic exit and cytokinesis, and SIN for cytokinesis [1,2]. In *S. cerevisiae*, Cdc15 kinase mediates the activation of the GTPase Tem1 to the downstream NDR kinase Dbf2 complexed with the regulatory subunit Mob1[3-5] (Fig. 1A). Although MEN and SIN are evolutionally conserved pathways, some differences have been noted in the composition, regulation and functional targets of the signalling components. For example, while Cdc15 kinase directly activates the NDR kinase Dbf2-Mob1 in MEN, activation of the equivalent SIN NDR kinase Sid2-Mob1

requires the sequential action of two kinases: first SpCdc7, which is the homologue of ScCdc15; second SpSid1 complexed with SpCdc14. [6]. No Sid1 homologue has been reported in either *S. cerevisiae*, *Ashbya gossypii,* or *Candida albicans*, the *Saccharomycetaceae* family members where the ME-signalling pathway has been investigated. In contrast, the filamentous fungus *Aspergillus nidulans* has a SIN-like pathway to regulate septation [7]. While the ultimate goal of MEN in *S. cerevisiae* is to activate Cdc14 phosphatase, the homologous Clp1 phosphatase is not the essential target of SIN in *S. pombe,* even though it is also regulated by SIN. The MEN components including Cdc15 have been studied in *Candida albicans* and the signalling pathway was demonstrated to be essential for mitotic exit and cytokinesis [8]. Interestingly, *CaCDC14* gene is not essential for growth [8,9]. When such divergences occurred during fungal evolution is not well understood.

Phenotypic analysis of gene knockout strains is important to elucidate the biological functions of a gene of interest. Recently, many non-conventional yeast species have been the subject of biological and applications research. Since the molecular toolboxes developed for the model yeasts are not always compatible, much effort has been made to develop suitable genetic tools, including for methylotrophic budding yeasts such as *Ogataea polymorpha* which is phylogenetically distant from *S. cerevisiae*, and has been used for industrial applications as well as biological research [10-12]. Although several strong constitutive as well as inducible promoters are available for *O. polymorpha*, these are not suited for cell cycle study. Efficient repression systems of gene function are needed in order to study essential genes expressed at normal endogenous levels. The inducible promoters that are currently available express genes at much higher than endogenous levels, which may cause some unwanted phenotypes in their ON states. Artificially designed inducible promoters such as theTet promoter, which can induce/repress gene expression by simply adding a specific compound into the medium, are ideal for biological studies because no changes in environmental conditions such as carbon sources and temperature are involved [13].

Proteolytic elimination of protein is another strategy to deplete protein levels in a cell. The auxin-inducible degron (AID) has proved to be a powerful tool to analyse the cellular function of essential and non-essential genes in various organisms [14,15]. It has been used in *O. polymorpha*, but worked well only for small number of genes[16] The modified AID system (AID2) that provide sharper degradation and higher sensitivity/specificity to the plant hormone auxin (indole-3-acetic acid, IAA) derivatives as well as the improved AID (iAID) system using the Tet promoter have been developed in *S. cerevisiae* and other organisms[17 18].

In this report, we identified two essential protein kinases, *OpHCD1* and *OpHCD2*, as components of the MEN/SIN kinase pathway in *O. polymorpha* that are homologues of Cdc7 and Sid1 in *S. pombe*. In order to obtain tools to construct conditional mutants in *O. polymorpha*, we employed strategies to improve auxin-degron system that were recently reported in *S. cerevisiae,* and applied these new methods to analyse the two kinases. Our results demonstrated that both OpHcd1 and OpHcd2 play important roles in mitotic exit and cytokinesis. The homologues of the second SIN kinase, SpSid1, are found in many budding yeast species and likely function in mitotic exit as well as cytokinesis.

Materials and Methods

Yeast strains and plasmids

Yeast strains and plasmids used in this study are listed in Table S1. Unless otherwise indicated, all *O. polymorpha* strains were derived from NCYC 495 and were generated by PCR-based methods [10,19,20]. *O. polymorpha* cells were transformed by electroporation [21]. To generate *hcd1*^{M80G} allele, primer OpHCD1_9 (ACCACCCAAAAACTCCCCAATAATCCACAGCTTGTATC) that encodes the M80G mutation was used to amplify the promoter region and a.a. 1-80 of *HCD1* ORF together with primer OpHCD1_7 (CGCTGCAGGTCGACGCGAGCATTTCGTCGATGAGG). A.a. 81-446 and the downstream terminator sequence was amplified with primers OpHCD1_10 (GAGTTTTTGGGTGGTGGATCC) and OpHCD1_8 (CTTAATTAACCCGGGACTTGCCGATCTCAGAGACC). These two DNA fragments were combined with BamHI digested pFA6a-natNT2 plasmid using NEBuilder HiFi DNA Assembly Master Mix (E2621, New England Biolabs, Ipswich, MA, USA). The resulting plasmid (pHM1119) was digested with Nsi1 and integrated at the *hcd1Δ* locus in HPH1737. The heterozygous diploid cells were transformed with Ku80+ plasmid (pHM898) and subjected to tetrad dissection to obtain a haploid clone carrying *hcd1Δ::hphNT1<<Ophcd1*^{M80G}*::natNT2*. Similarly, the *hcd2*^{L215G} plasmid (pHM1121) was constructed with primers OpHCD2_7 (CGCTGCAGGTCGACGTTCCATGCGAACCACAGAAG), OpHCD2_8 (CTTAATTAACCCGGGCAATACGAAGACTAGCAGCC), OpHCD2_9 (ACTTTCGCAGTATTCGCCTATCAAATTCATAGACATCTCG), and OpHCD2_10 (GAATACTGCGAAAGTGGCTC). The pHM1121 DNA was digested with StuI, and used to transform HPH1738 by integrating it at the *hcd2Δ* locus. The heterozygous diploid cells were transformed with pHM898 and subjected to tetrad dissection to obtain a haploid clone carrying *hcd2Δ::hphNT1<<Ophcd2*^{L215G}*::natNT2.* To construct iAID plasmids, OsTIR-9myc, TetR, mAID, TetR-VP16 hybrid transactivator (tTA) gene-tetO7, spacer-5xflag, and hphNT1 fragments were PCR amplified from pNHK53, pST1760, pST1872 (obtained from NBRP Yeast), pCM225 [22], pKL260 (a kind gift from M. Kanemaki), and pFA6a-hphNT1[20]respectively. *OpURA3*, *OpLEU1*, *OpADE12* fragments including the ORF and 5'-upstream as well as 3'-downstream regions, *OpADH1* promoter, *OpTEF1* promoter and

terminator, *OsSSN6* ORF (scaffold_1: 94041-96002) were amplified from *O. polymorpha* genome. These fragments were combined in pRS305 to generate iAID plasmids. The schematics and sequences of these plasmids used in this study are listed in Table S2.

Yeast growth conditions and general methods

Yeast strains were grown either in YPD medium containing 200 mg/L adenine, leucine, and uracil (YPDS) or in synthetic/defined (SD) medium supplemented with appropriate amino acids and nucleotides [23]. Cells were grown at 30°C unless otherwise indicated. IAA (Merck KGaA, Darmstadt, Germany), 5-Ad-IAA (A3390, Tokyo Chemical Industry Co., Tokyo, Japan), 5-Ph-IAA (BioAcademia, Osaka, Japan), were dissolved in ethanol for IAA, or DMSO for 5-Ad-IAA and 5-Ph-IAA to make a 500 mM stock solution and stored at -20°C. To induce degradation of the endogenous protein fused with mAID, IAA, 5-Ad-IAA, or 5-Ph-IAA was added directly to the culture medium at the indicated concentration. Doxycycline (Takara Bio Inc., Shiga, Japan) was dissolved in H_2O at 10 mg/ml and stored at -20°C.

Microscopy

To visualize DNA, yeast cells were fixed in 70% ethanol, washed with phosphate-buffered saline (PBS), and incubated in PBS containing 1 µg/ml 4'6,-diamidino-2-phenylindole (DAPI). DAPI images were acquired using an ECLIPSE Ti2-A inverted microscope (Nikon) equipped with a CFI Plan Apo Lambda 100 × objective lens (1.45 numerical aperture), a DS-Qi2 digital camera, an LED-DA/FI/TX-A triple band filter (Semrock: Exciter, FF01-378/474/575; Emission, FF01-432/523/702; Dichroic mirror, FF409/493/596-Di02), an LED light source X-LED1 and differential interference contrast (DIC) for DAPI, or BZ-700 with a PlanApo 60x objective lens (Keyence Co., Osaka, Jpan). To observe GFP-Tubulin signal, Z-series images of 0.4µm steps were captured without fixation using a DeltaVision microscope (Applied Precision, Issaquah, WA, USA) equipped with GFP and TRITC filters (Chroma Technology Corp., Bellows Falls, VT, USA), a 100× NA 1.4 UPlanSApo oil immersion objective (IX71; Olympus, Tokyo, Japan), and a camera (CoolSNAP HQ; Roper Scientific, Trenton, NJ, USA), or BZ-700 with a PlanApo 60x objective lens after fixing in 4% formaldehyde for 20 min. Images were analysed/processed with SoftWoRx 3.5.0 (Applied Precision, Issaquah, WA, USA), Prism4.3.0 software [24], or ImageJ 1.47 (NIH, Bethesda, MD,

USA). Adobe Photoshop (Adobe Systems, Inc., San Jose, CA, USA) and Affinity Photo 1. 8.4 (Serif (Europe) Ltd, Nottingham, UK) were used to assemble images for figures.

RNA analysis

Total RNA was isolated from *O. polymorpha* as previously described[25], treated with DNase I, and then further purified using the Monarch Total RNA Miniprep Kit (New England Biolabs, Ipswich, MA, USA). A total of 250 ng RNA was used to synthesize cDNA with Reverse Tra Ace qPCR RT Master Mix (Toyobo Co., Ltd., Osaka, Japan) according to the manufacturer's protocol, and a 0.1-0.5 µl cDNA reaction mixture was used in qPCR reactions. Primers ACT1_8 (CTTCTTCCCAGTCTTCTGCTATC) and ACT1_9 (GGGCTCTGAATCTCTCATTACC) were used to amplify ACT1 RNA, and primers SPC72_Fw (ATGGCTGACCAAATCCTAGAC) and SPC72_Rv (GCTCTCAACTTTGCACTTAACC) for SPC72 RNA.

Yeast cell extract and immunoblotting

Whole cell extracts were prepared for SDS-PAGE and immunoblotting [20,26 27]. Samples representing 1–2 OD600 of liquid culture were resuspended in 950 µl of cold 0.29 M NaOH and incubated on ice for 10 min. Then, 150 µl 55% (w/v) trichloroacetic acid was added and incubated for 10 min on ice. Protein pellets were collected by removing the supernatant after centrifugation at 14,000 rpm for 15 min at 4°C, then resuspended in high urea buffer (8 M urea, 5% SDS, 200 mM $NaPO_3$ pH 6.8, 0.1 mM EDTA, 100 mM dithiothreitol, and bromophenol blue) and heated at 65°C for 10 min before loading on a gel. Western blotting was performed using a standard protocol. M2 monoclonal antibody (F1804, Sigma) and rabbit anti-mouse antibodies (ThermoFisher Scientific) were used to detect flag-tagged proteins. GE Healthcare Amersham™ ECL Prime Western Blotting Detection Reagent

Results and Discussion

OpHCD1 and *OpHCD2* encode kinases similar to *S. pombe* SIN kinases

A BLAST search of *O. polymorpha* genome sequence using *S. cerevisiae* MEN components (Tem1, Cdc15, Dbf2, Mob1, Lte1, Ste20, Bub2, and Bfa1) as query sequences identified homologues of all proteins except *ScCDC15* (Fig. S1). Since ScCdc15 is a member of the Ste20 family of protein kinases, we suspected that one of Ste20-like kinases may be a functional homologue and looked more closely at the hits in the BLAST search using the ScCdc15 amino acid query sequence. Among the top six hits, two ORFs had no obvious homologues in *S. cerevisiae*, and were named *OpHCD1* and *OpHCD2* (*homologue candidate of ScCdc15*). We performed a phylogenetic analysis of OpHcd1, OpHcd2 and the 4 other top hits from *O. polymorpha* proteins along with the five proteins closest to either OpHcd1 or OpHcd2 in *S. cerevisiae* as well as the 8 closest in *S. pombe* (Fig. 1B). The results showed that OpHcd1 and OpHcd2 have similarity to ScCdc15, SpSid1 and SpCdc7. OpHcd2 displays 22% identity (35% similarity) to ScCdc15, and 21% identity (34% similarity) to SpCdc7. OpHcd2 has a protein kinase domain near the N-terminus, and in addition contains an armadillo type fold in the C-terminal region similar to SpCdc7 (Fig. 1C). OpHcd1 is smaller in size (446 amino acids) and shows only 15% identity (22% similarity) to ScCdc15, but the amino acid identity is higher to SpSid1 (38% identity and 55% similarity) (Fig. 1C). Thus, these analyses suggested that OpHcd2 is the homologue to ScCdc15/SpCdc7 and OpHcd1 to SpSid1. Since a Sid1 homologue has not been reported in budding yeasts, we extended the BLAST search to other species in *Ascomycota*. Budding yeast species that diverged from the *S. cerevisiae* linage at early stages of evolution have an *OpHCD1*/*Spsid1* homologue gene in addition to *ScCDC15* homologue in their genomes, while the *S. cerevisiae* linage has lost it after the split with the *Wickerhamomyces* linage (Fig. 1D). These results suggested that OpHcd1 and OpHcd2 are orthologs of SpCdc7 and SpSid1 and may play roles in late mitosis in *O. polymorpha*, and that the ancestral SIN-like signalling pathway has lost the Sid1 kinase relatively recently in budding yeast evolution.

OpHcd1 plays roles in mitosis and cytokinesis

To investigate cellular functions of *OpHCD1* and *OpHCD2*, we first constructed deletion mutants. Heterozygous *hcd1 Δ::hphNT1/HCD1* diploid cells were subjected to tetrad analysis, where the four spores of each ascus were analysed for the ability to grow on rich and selective plates. All asci formed one or two colonies (Fig. 2A). None of those growing were positive for the resistance marker (hygromycine) corresponding to the *hcd1 Δ::hphNT1* deletion allele, while the segregations of heterologous auxotrophic *leu1-1* and *ura3-1* alleles were consistent with random segregation (*LEU1*:*leu1-1*=8:2, *URA3*: *ura3-1*=6:4 in 5 tetrads) (Fig. 2A). Similar results were obtained in the tetrad analysis of heterozygous *hcd2 Δ::natNT2/HCD2* diploid cells, where *HCD2* was deleted using nourseothricin (nat) resistance marker (Fig. 2B): no nat resistant colonies were obtained while auxotrophic markers were segregated close to randomly (*LEU1*:*leu1-1*=7:7, *URA3*: *ura3-1*=6:8 in 7 tetrads). Thus, both *OpHCD1* and *OpHCD2* genes are essential for growth in *O. polymorpha*. Spores that were presumed to carry *hcd1 Δ* or *hcd2 Δ* allele did not form micro-colonies after prolonged incubation. Spores were germinated, although the number of cell bodies varied from spore to spore, and we were unable to determine whether the cells have a defect in cell cycle progression.

Mutating the conserved "gatekeeper" residue in the ATP-binding pocket of protein kinases to glycine enlarges the pocket so that PP1 analogs such as 1NM-PP1 can occupy it and inhibit the kinase activity [28]. Since the ATP analog-sensitive (as) allele of *ScCDC15* causes anaphase arrest in the first cell cycle after the drug addition, we introduced the equivalent mutation into *OpHCD1* and *OpHCD2* (Fig. S2) [29]. The growth of $hcd1^{M80G}$ (hereafter called *hcd1-as*) cells was reduced on Yeast Extract–Peptone–Dextrose (YPD) solid medium containing 0.5 μM 1-NM-PP1, and almost abolished at 5 μM, therefore we used the *hcd1-as* allele for the phenotypic analysis of *OpHCD1* (Fig. 2C). In contrast, $hcd2^{L215G}$ (hereafter called *hcd2-as*) cells did not show any growth defect in the presence of 1NM-PP1 on YPD plates (Fig. 2C).

To investigate cellular functions of OpHcd1, logarithmically growing *hcd1-as* cells were treated with 1NM-PP1 and both cell division and cellular morphology were examined over time (Fig. 3A, B). The proportion of unbudded G1 cells was reduced (Fig. 3C), whilst the proportion of large budded cells with two nuclei, corresponding to anaphase and telophase cells, was increased from 17.5 % to 32.9 % after 1 hour incubation with 1NM-PP1 (Fig. 3D), suggesting defects in late mitotic progression. After a two hour-incubation, cells which had initiated budding of the next cell cycle without completion of cytokinesis and/or

cell separation in the previous cell cycle became evident (Fig. 3B and 3D). To clarify whether *hcd1-as* cells have defects in mitotic exit, *hcd1-as* cells expressing GFP-Tub1 (encoding for tubulin for spindle visualization) were analyzed. The proportion of *hcd1-as* cells with fully elongated anaphase spindles strongly increased after 2 hours of 1NM-PP1 treatment compared to wild type cells (Fig. 3E). Furthermore, some cells with a small bud were still attached to a neighboring cell (Fig. 3F). GFP-Tub1 patterns indicated that both the cell with the small bud and its neighboring cell were in interphase. However, the cytoplasmic GFP signals were continuous between the two cells, suggesting that these cells were the mother and daughter cells from the previous cell cycle and that cytokinesis was still incomplete. These results suggested that OpHcd1 plays a role in mitotic exit as well as in cytokinesis and/or cell separation that are difficult to firmly distinguish by the method used.

Even though there was no obvious growth defect on YPD plates, the *hcd2-as* cells transiently accumulated late mitotic cells in the time course experiment, which suggests the Hcd2-as protein is partially sensitive to 1NM-PP1 (Fig. S3).

The iAID system is a new genetic tool for constructing conditional mutants in *O. polymorpha*

In order to analyse the consequences of OpHcd2 loss for cell division, we next considered conditional depletion of OpHcd2 protein. Previously, we used the AID system in *O. polymorpha* to generate a conditional *OpCDC5* mutant, which encodes the essential polo-like kinase. However, the C-terminal AID tagging did not work well for *OpHCD2* gene (Fig. S4). Therefore, we attempted to establish a more efficient gene depletion method that is widely applicable in *O. polymorpha*. Firstly, we employed the improved AID system in *S. cerevisiae*, iAID, where the Tet-OFF transcriptional repression system was combined with the existing AID system [18]. Since the antibiotic resistant marker units commonly used in *S. cerevisiae* were functional in *O. polymorpha*, we expected that the Tet-OFF system of *S. cerevisiae* might work in *O. polymorpha.* We then tested the Tet-OFF system for *OpCDC5*, *OpSPC72*, and GFP genes (Fig. 4A). The *OpCDC5-flag* gene was placed under the Tet promoter for *S. cerevisiae*, which consists of TetO7 repeats and *ScCYC* tata sequence, and the resulting plasmid was integrated into the *O. polymorpha* genome together with the tetracycline-controlled TetR-VP16 hybrid transactivator (tTA) gene. Cdc5-flag protein was not detected in cells growing in YPD medium without doxycycline (promoter ON) by Western blotting using anti-flag antibody, suggesting the gene was not expressed (Fig. 4A, TetO7-

303 *ScCYC1*tata-*OpCDC5-flag*). We then replaced the *ScCYC1* tata sequence with a tata like
304 sequence in the upstream region of *OpACT1* gene (TetO7-*OpACT1*tata) (Fig. S5). When
305 placed under TetO7-*OpACT1*tata, the Cdc5-flag protein was expressed efficiently in all four
306 independent clones (Fig. 4A). Thus, the P_{TetO7}-*OpACT1*tata promoter has a promoter activity
307 in *O. polymorpha,* and hereafter we refer to it as P_{TetO7} or the TetO7 promoter.
308 The addition of doxycycline in YPD medium alone did not lower the Cdc5-flag
309 protein level expressed from the TetO7 promoter. In *S. cerevisiae*, introduction of *ScSSN6* or
310 *ScTUP1* fused with the reverse Tet repressor (TetR') is necessary for tight regulation because
311 of the leaked expression under the repressed conditions [30]. We identified the *ScSSN6*
312 homologue in *O. polymorpha* genome (scaffold_1: 94041-96002) and introduced P_{TEF1}-
313 TetR'-*OpSSN6-flag* fusion gene into *O. polymorpha* wild type cells. Then, the plasmids
314 carrying P_{TetO7}-*OpCDC5-flag*, P_{TetO7}-*OpSPC72-flag*, or P_{TetO7}-GFP-flag were integrated into
315 the genome and the flag-tagged protein were examined in the presence of doxycycline at
316 different concentrations (Fig. 4B, Fig. S6A). In comparison to control conditions (without
317 doxyclycine), Cdc5-flag and Spc72-flag proteins were lower in the presence of 0.25 µg/ml or
318 1 µg/ml doxycycline decreasing to 52 % and 57 % of control levels, respectively. Further
319 increasing doxycycline concentration up to 100µg/ml did not improve the repression of
320 OpCdc5 or OpSpc72 (Fig. S6B). To verify doxycycline-dependent repression of transcription,
321 we analysed the RNA level of the *OpSPC72* gene in cells carrying P_{TetO7}-*OpSPC72-flag,* tTA,
322 and P_{TEF1}-TetR'-*OpSSN6-flag* by quantitative RT-PCR using *OpSPC72* specific primers. The
323 RNA level of *OpSPC72* was reduced after 7 hours incubation in the presence of doxycycline,
324 but only by 34 % (Fig. 4C). Endogenous *OpSPC72* RNA may be the reason for the
325 inefficient repression of the *OpSPC72* RNA level.
326 Next, we combined the TetO7 promoter with the AID system. Wild type cells
327 expressing either P_{TetO7}-*OpCDC5-flag* or P_{TetO7}-mAID-*OpCDC5-flag* together with tTA,
328 P_{TEF1}-TetR'-*OpSSN6*, and P_{ADH1}-*OsTIR* (the auxin receptor F-box protein Trans-port
329 Inhibitor Response1 from Oryza sativa, OsTIR) were grown in YPD medium containing IAA
330 and/or doxycycline, and the flag-tagged proteins were examined by Western analysis using
331 anti-flag antibody (Fig. 4D and Fig. S7). While the Cdc5-flag protein levels were reduced by
332 only ~20-40%, the mAID-Cdc5-flag protein was depleted by ~80 % (Fig. 4D and Fig. S7).
333 Thus, the iAID strategy improved the efficiency of the AID system in *O. polymorpha.*
334
335
336 **iAID-*Ophcd2-as* cells exhibit defects in mitotic exit and cytokinesis**

We then applied the iAID system to the *OpHCD2* gene. The plasmid carrying P_{TetO7}-mAID-*Ophcd2-as* and tTA was inserted at the *OpURA3* locus in *hcd2Δ*/+ heterologous diploid cells carrying P_{ADH1}-*OsTIR* and P_{TEF1}-*TetR'-OpSSN6* (Fig. S8A). Meiosis and sporulation was induced, and a haploid strain with the genotype P_{TetO7}-mAID-*hcd2-as* *Δhcd2* P_{ADH1}-*OsTIR* P_{TEF1}-*TetR'-SSN6* was obtained by tetrad dissection (hereafter referred to as iAID-*hcd2-as*). The iAID-*hcd2-as* cells grew normally on YPD medium, but the growth was slower and reduced on YPD medium containing IAA, doxycycline, and 1NM-PP1 compared with either cells expressing the wild type *OpHCD2* gene or without *OsTIR* expression (Fig. S8B and S8C). To further improve the tightness of the mutant, *OsTIR* was replaced by the mutant versions $OsTIR^D$ and $OsTIR^A$ that give higher sensitivity and specificity to IAA derivatives in various organisms including *S. cerevisiae* [31]. The $OsTIR^A$ version of the iAID-*hcd2-as* allele (iAID2-*hcd2-as*) conferred a tighter growth-defective phenotype in the presence of auxin derivatives that have high affinity to $OsTIR^D$ and $OsTIR^A$, 5-Ph-IAA or 5-Ad-IAA, at ≥1 μM compared to wild type *OsTIR* with 500 μM IAA (Fig. 5A). Wild type and iAID2-*hcd2-as* cells expressing $OsTIR^A$ were grown to log phase in YPD medium, when 5-Ad-IAA, doxycycline, and 1NM-PP1 were added and the cells incubated for a further 2 h, then cell morphology and DNA were examined by microscopy (Fig. 5B and 5C). In iAID2-*hcd2-as* cells, the percentage of unbudded G1 cells decreased after 1 h and remained low ($p<0.05$, Friedman test), suggesting that the cell cycle was delayed or arrested, while it did not change significantly in wild type cells ($p=0.19$, Friedman test) (Fig. 5C, upper graphs). Instead, after 1h anaphase/telophase cells (large budded cells with two segregated nuclei) increased to 58.0 % in iAID2-*hcd2-as* cells ($p<0.05$, Friedman test), but not in wild type cells ($p=0.50$, Friedman test) (Fig. 5C, lower graphs). Longer incubation time did not increase the proportion of anaphase/telophase cells, but instead led to the appearance of cells with more than three cell bodies that remained connected (Fig. 5C, purple), indicating cytokinesis defects. To confirm the phenotype, GFP-Tub1 was expressed in wild type and iAID2-*hcd2-as* cells and the cell cycle stages present were determined up to 2h incubation time. In iAID2-*hcd2-as* mutants the proportion of cells containing anaphase spindles had increased by 1 h after the addition of 5-Ad-IAA, doxycycline, and 1NM-PP1, but did not exceed 50% (Fig. 5D and 5E). On further incubation up to 2 hours total, the proportion of anaphase cells had slightly decreased. Instead chains of cells appeared, which had three or more unseparated cell bodies in various cell cycle stages based on the GFP-tubulin distribution and structures. Close

inspection of cytoplasmic GFP signals in such cells revealed that the cytoplasm between the cell bodies was often but not always continuous, suggesting possible defects in cytokinesis. However, it is difficult to distinguish cells that have not completed cytokinesis from those with cell separation defects solely by the cytoplasmic GFP signal. Thus, these results suggested that the depletion of OpHcd2 delayed mitotic exit as well as cytokinesis and/or cell separation.

In this study, we investigated the phenotypes of conditional mutants for *OpHCD1* and *OpHCD2* that encode protein kinases similar to the SIN kinases, SpCdc7 and SpSid1 in *S. pombe*. Both the *hcd1-as* and iAID2-*hcd2-as* mutants exhibited similar phenotypes with a delay of mitotic exit and cytokinesis/cell separation defects. These results suggested that OpHcd1 and OpHcd2 are likely components of an MEN/SIN-homologous signaling pathway in *O. polymorpha* and play important roles in mitotic exit and cytokinesis. Because *hcd1-as* and iAID2-*hcd2-as* cells only transiently arrested the cell cycle in anaphase during time-course experiments, we assume that these conditional mutant alleles have some leakiness in liquid media, even though they exhibited severe growth defect on solid medium under restrictive conditions. It is unclear why the analog-sensitive mutation made the Hcd2 protein sensitive to 1NM-PP1 but was insufficient for the construction of a conditional mutant. It is known that cells can tolerate the reduced activity of several kinases [28]. Lower levels of Hcd2 activity may be sufficient for cell division.

The MEN in *S. cerevisiae* and the SIN in *S. pombe* are equivalent signalling pathways. However, they diverge in their detailed signalling architecture and roles in the cell cycle. While the activation of the GTPase in the MEN is transduced to the most downstream NDR kinase Dbf2-Mob1 through a single kinase, Cdc15, the SIN requires two kinases. Phylogenetic evidence clearly indicates that the SIN type is the ancestral form and the loss of the second kinase occurred more recently in budding yeast evolution (Fig. 1D). The significance of having the second kinase in the pathway is not understood. The MEN-type signalling composition may simply have altered the regulatory mechanism to compensate and bypass the requirement for the second kinase. However, it may be possible that the MEN-type had a functional advantage over the SIN-type for the budding style of cell division. Importantly, ScCdc15 is a simultaneous detector for both the Tem1 activation, which occurs when one nucleus entre into the daughter cell body (spatial), and the Cdc5 kinase activity, which is high during mitosis (temporal), to ensures that mitotic exit occurs only after the completion of nuclear division and segregation [32]. As for the SIN, how the kinases are regulated and which kinase senses signals such as cell cycle stages, environmental

404 information, are not understood. It may be reasonable to speculate that Cdc15 in *S. cerevisiae*
405 inherits functions of both kinases in the SIN-like pathway and became a merging point of
406 different signals that had separate target kinase to modulate the SIN-type pathway. Further
407 study will be required to determine whether the MEN-type architecture has advantages in the
408 budding yeast cell division. Understanding which signalling components are regulated by
409 spatial and temporal signals in *O. polymorpha* may help clarify the roles of each kinase in the
410 SIN-type pathway.
411 While the SIN in *S. pombe* primarily regulates cytokinesis, the MEN in *S. cerevisiae*
412 is essential for mitotic exit and cytokinesis. Similarly to the MEN, the pathway in *C. albicans*
413 plays key roles in driving mitotic exit, cytokinesis, and cell separation. In *S. cerevisiae*, all
414 core components of the MEN are essential for signalling to activate the downstream Cdc14
415 phosphatase and thus common phenotypes are shared among their mutants. In contrast, in *C.*
416 *albicans*, mutants of core components exhibited diverse phenotypes. Thus each component
417 may have distinct roles to achieve the cellular functions of the ME-signalling pathway:
418 CaTem1 and CaCdc15 for mitotic exit, CaDbf2 primarily for cytokinesis, and the non-
419 essential CaCdc14 for cell separation. It is unclear whether the divergent roles of each of the
420 signalling components is unique to *C. albi*cans and related to its ability to switch the
421 morphological forms of growing cells from yeast form to pseudo-hyphae or true hyphae; or
422 alternatively this diversity of roles is common among other budding yeast species in
423 Saccharomycetaceae. The results of this study suggest that the regulation of mitotic exit was
424 placed under the ME-signalling pathway during the evolution of Saccharomycetaceae.
425 Further analysis on other components of the ME-signalling pathway in *O. polymorpha* will
426 shed light on the conservation and divergence of the roles and regulation of each component
427 of the ME-signalling pathway in yeasts.
428

Acknowledgements

We thank Dr. S. Tanaka for technical advice, National BioResource Project Yeast for materials, the Research Support Center, Research Center for Human Disease Modeling, Kyushu University Graduate School of Medical Sciences for technical support. We are grateful to Drs. J. Kanoh and Y. Higuchi for their support, and Dr. D. Drummond for critical reading of the manuscript. The work was supported by JSPS Scientific Research (C) JP19K06641, Initiative for Realizing Diversity in the Research Environment, a grant from Institute for Fermentation Osaka, and a grant from Noda Institute for Scientific Research to H.M., and Initiative for Realizing Diversity in the Research Environment to Kyushu University.

Author Contributions

Conceived the project: HM. Designed and carried out the experiments: HM, SJ. Analysing the data: HM, SJ, GP, KT. Wrote the manuscript: HM, SJ, GP.

Competing Interests

The authors declare that they have no competing interests.

Figure legends

Figure 1 *OpHCD1* and *OpHCD2* encode protein kinases homologous to Sid1 and Cdc7 in *S. pombe*.

(A) Schematics of the core components of the MEN and SIN and the homologous pathway in *O. polymorpha*. The protein IDs for *O. polymorpha* proteins are according to the reference 30.

(B) Phylogenetic tree of protein kinases from *S. cerevisiae, O. polymorpha*, and *S. pombe* that have similarity with *S. cerevisiae* Cdc15.
Phylogenetic tree was constructed in MEGAX with the Maximum Likelihood Method. Shown is the Bootstrap Consensus Tree.
(C) Schematic representation of the OpHcd1, OpHcd2, ScCdc15, SpCdc7, and SpSid1 proteins. Blue and green boxes are the protein kinase domain and the armadillo type fold, respectively. The numbers are from the amino acid identity alignment between two kinases across the length of the proteins.
(D) Conservation of ScCdc15/SpCdc7 and SpSid1 in Ascomycota. Phylogenetic relationships are based on Shen et. al [33]. Tree is not in scale.

Figure 2 *OpHCD1* and *OpHCD2* are essential for growth
(A) Tetrad analysis of heterozygous *hcd1 Δ /+* diploid cells (HPH1834). Cells were incubated on an MAME sporulation plate before dissection of spores. Two or fewer colonies were formed in all tetrads.
(B) Tetrad analysis of heterozygous *hcd2 Δ /+* diploid cells (HPH2251). Cells were incubated on an MAME sporulation plate before dissection of spores. Two or fewer colonies were formed in all tetrads.
(C) Growth assay of the *hcd1-as* and *hcd2-as* mutants. Serial dilutions of wild type (HPH954), *hcd1-as* (HPH1894), and *hcd2-as* (HPH1909) strains were spotted on YPDS agar plates containing the indicated concentration of 1NM-PP1 and incubated at 30 °C.

Figure 3 *Hcd1-as* cells have defects in mitosis and cytokinesis
(A) Logarithmically growing wild type (HPH1047) and *hcd1-as* (HPH1894) cells in YPDS medium were incubated with 5 μM 1NM-PP1 at 30 °C for 1 hrs. Cells were fixed with 70% ethanol and DNA was stained with DAPI. Merged image combines DAPI fluorescence and brightfield. Scale bar, 10 μm.
(B) DAPI image of *hcd1-as* in the same experiment as in (A). Cells were fixed after 2 hrs. Asterisks indicate unseparated cells. Scale bar, 10 μm.
(C, D) Quantification of A and B. C: percentage of unbudded cells with one nucleus. D: percentage of large budded cells with two nuclei, one in the mother and the other in the bud, and unseparated large cell bodies with two or more nuclei. More than 100 cells were analysed

493 at each time point. The experiment was performed in triplicate and the combined results are
494 shown.
495 (E) Logarithmically growing wild type (HPH1968) and *hcd1-as* (HPH1969) cells carrying
496 *GTP-TUB1* in YPDS medium were incubated with 5 μM 1NM-PP1 at 30 °C for 2 hrs.
497 Images were captured without fixation. Bright field image and GFP fluorescence image are
498 merged. Shown are projected images. Scale bar, 5 μm.
499 (F) Incomplete cytokinesis and cell separation of *hcd1-as* cells from the experiment in E.
500 Asterisks indicate newly formed buds. White arrows point the connections between mother
501 and daughter cells of the last cell cycle. Scale bar, 2 μm.
502
503 Figure 4 The iAID system in *O. polymorpha*
504 (A) Cdc5 protein levels expressed from the modified Tet promoters. Cdc5-5flag protein was
505 exogenously expressed from TetO7-TATA$_{ScCYC1}$ promoter or TetO7-TATA$_{OpACT1}$ promoter
506 in wild type cells expressing TetR-VP16. Total cell extracts were prepared and subjected to a
507 western analysis using anti-flag antibody. Three and four independent clones of HPH1942
508 and HPH1943, respectively, were analysed. No plasmid: wild type cells not carrying the
509 OpCDC5-5flag plasmid (HPH656).
510 (B) Cdc5-5flag, Spc72-5flag, or GFP-5flag protein level expressed from the Tet promoter in
511 the presence of doxycycline. CDC5-5flag (HPH2004), SPC72-5flag (HPH2008), or GFP-
512 5flag (HPH2009) genes were placed under TetO7-TATA$_{OpACT1}$ promoter in wild type cells
513 carrying P$_{CMV}$-tTA, P$_{OpTEF1}$-*TetR'-OpSSN6-5flag*. Cells were pre-cultured in YPDS at 30 °C,
514 then doxycycline was added at the indicated concentration and incubated for 5 hrs at 30 °C.
515 Total cell extracts were prepared and subjected to a western analysis using anti-flag antibody.
516 Note that the two slowest migrating bands correspond to the TetR'-Ssn6-5flag. No-tag: wild
517 type (HPH951). Intensity of bands was quantified with ImageJ software.
518 (C) The *SPC72* RNA expression level. Wild type cells carrying P$_{TetO7}$-*OpSPC72-5flag*, tTA,
519 and P$_{OpTEF1}$-*TetR'-OpSSN6-5flag* (HPH2008) were grown in YPDS. Doxycycline was added
520 at indicated concentration and cells were incubated at 30 °C for 7 hrs. Total RNAs were
521 subjected to qRT-PCR analysis for *SPC72* RNA and *ACT1* RNA. Relative expression to that
522 without doxycycline was calculated. The experiment was performed in triplicate and the
523 combined results are shown.
524 (D) Cdc5 protein level expressed by the iAID system. Wild type diploid cells carrying either
525 P$_{TetO7}$-*CDC5-5flag* (HPH2044) or P$_{TetO7}$-*mAID-CDC5-5flag* (HPH2046) as well as P$_{ADH1}$-
526 *OsTIR*, P$_{CMV}$-tTA, P$_{OpTEF1}$-*TetR'-OpSSN6-5flag* and wild type haploid cells were grown in

SD medium supplemented with appropriate nucleotide and amino acids in the presence or absence of 20 mg/ml doxycycline. IAA and 1NM-PP1 were added at 0.5 mM and incubated at 30 °C for 2.5 hrs. Total cell extracts were prepared and subjected to a western analysis using anti-flag antibody. Intensity of bands was quantified with ImageJ software. Similar result was shown in Fig. S5.

Figure 5 OpHcd2 depleted cells are defective in mitotic exit and cytokinesis

(A) Serial dilutions of strains with the indicated genotype were spotted on YPDS agar plates containing IAA, 5-Ph-IAA, or 5-Ad-IAA at the indicated concentrations and incubated at 30 °C for 1day. Yeast strains: HPH656, HPH2067, HPH2254, HPH2246, HPH2270, HPH2244, HPH2245, HPH2247.

(B) DAPI staining of iAID2-*hcd2-as* strains. Wild type (HPH2247) and iAID2-*hcd2-as* cells (HPH2245) carrying P_{ADH1}-*OsTIR*^{A}, P_{CMV}-tTA, P_{OpTEF1}-*TetR'-OpSSN6-5flag* were grown in YPDS medium until logarithmic growth phase. Dox, IAA, and NM-PP1 were added at 5 µg/ml, 0.5 mM, and 5µM, respectively, and incubated at 30 °C for up to 2 hrs. Cells were fixed with 70 % ethanol and DNA was stained with DAPI. Shown are merged images of bright field and DAPI images. Scale bar, 10 µm. Arrows indicate failure of cell separation in the previous mitosis.

(C) Quantification of B. Upper graphs: percentage of unbudded cells with one nucleus. Lower graphs: percentage of large budded cells with two nuclei, one in the mother and the other in the bud, and unseparated three or more cell bodies with two or more nuclei.

(D) GFP-tubulin was examined by epifluorescence microscopy in wild type and iAID2-*hcd2-as* strains. Wild type (HPH2258) and iAID2-*hcd2-as* cells (HPH2260) carrying P_{ADH1}-*OsTIR*^{A}, P_{CMV}-tTA, P_{OpTEF1}-*TetR'-OpSSN6-5flag* and expressing *GFP-TUB1* were grown in YPDS medium until logarithmic growth phase. Dox, IAA, and NM-PP1 were added at 5 µg/ml, 0.5 mM, and 5µM, respectively, and incubated at 30 °C for up to 2 hrs. Cells were fixed with 4% formaldehyde for 20 min and washed with PBS before microscopy. Asterisks indicate anaphase spindle. Shown are merged images of bright field image and DAPI image. Scale bar, 5 µm.

(E) Quantification of D. Upper graphs: percentage of unbudded G1 cells. Lower graphs: percentage of budded cells with anaphase spindle and unseparated three or more cell bodies without anaphase spindle.

(F) Incomplete cytokinesis and cell separation of iAID2-*hcd2-as* cells from the experiment in E. Asterisks indicate newly formed buds. Yellow and white arrows point the complete

561 separation and the connection between mother and daughter cells of the previous cell cycle,
562 respectively. Brightfield (left) and epifluorescence (GFP) (right) image. Scale bar, 2 µm.

Supplemental materials

Table S1. Yeast strains and plasmids.

Table S2. iAID plasmids for *O. polymorpha*.

Figure S1. Result of BLAST search using blastp for *O. polymorpha* model proteins at the genome portal of the Department of Energy Joint Genome Institute (https://mycocosm.jgi.doe.gov/Hanpo2/Hanpo2.home.html) [34].

Figure S2. Amino acid alignments of OpHcd1, OpHcd2, ScCdc15, SpCdc7, and SpSid1. Amino acid sequences of OpHcd1, ScCdc15, and SpSid1 (A) or OpHcd2, ScCdc15, and SpCdc7 (B) were aligned with MafftWS by Jalview 2.8.2 [35]. Asterisks indicate the position of the amino acid of ScCdc15 whose mutation to glycine caused the ATP-analog 1NM-PP1 sensitivity.

Figure S3. *hcd2-as* cells transiently accumulated late mitotic cells after addition of 1NM-PP1 Logarithmically growing wild type (HPH2186) and *hcd2-as* (HPH1870) cells in YPDS medium were incubated with 5 μM 1NM-PP1 at 30 °C. Cells were fixed with 70% ethanol and DNA was stained with DAPI. The graph shows the percentage of large budded cells with two nuclei, one in the mother and the other in the bud, which represents the late mitotic stage. More than 100 cells were analysed at each time point.

Figure S4. Growth assay of the *hcd2-mAID* mutant.
Serial dilutions of wild type (HPH1319), *hcd2-mAID* (HPH1599, HPH1600) strains were spotted on YPDS agar plates containing the indicated concentration of IAA and incubated at 30 °C.

Figure S5. Promoter region of *OpACT1* gene.
(A) Schematic map of the DNA sequence surrounding *OpACT1* gene (scaffold_5:1,140,451..1,142,929) drawn with SnapGene (GSL Biotech LLC). The DNA

595 sequence was obtained at the genome portal of the Department of Energy Joint Genome
596 Institute (https://mycocosm.jgi.doe.gov/Hanpo2/Hanpo2.home.html) [34]
597 (B) Genomic nucleotide sequence of *OpACT1* gene and the upstream region. Dark grey
598 boxes with bold letters are exons 1-3. Itallics in a grey box is the TATA-like sequence used
599 in Tet-OFF system for *O. polymorpha.* Light grey marks the upstream ORF.
600
601 Figure S6 Tet-OFF system in *O. polymorpha*
602 (A) Schematic maps of the plasmids used to construct the *OpCDC5* Tet-OFF strain. Both
603 pHM1129 and pHM1133 plasmids were integrated into *OpURA3*. The maps were drawn with
604 SnapGene.
605 (B) Cdc5-5flag and Spc72-5flag protein level expressed from the Tet promoter in the
606 presence of doxycycline. *CDC5*-5flag (HPH2004) and *SPC72*-5flag (HPH2008) genes were
607 placed under TetO7-TATA$_{OpACT1}$ promoter in wild type cells carrying P$_{CMV}$-tTA, P$_{OpTEF1}$-
608 *TetR'-OpSSN6-5flag*. Cells were pre-cultured in YPDS at 30 °C, then doxycycline was added
609 at the indicated concentration and incubated for 5 hrs at 30 °C. Total cell extracts were
610 prepared and subjected to a western analysis using anti-flag antibody. Wild type cells
611 carrying P$_{OpTEF1}$-*TetR'-OpSSN6-5flag* (HPH1926) was used as the negative control. Note that
612 the two slowest migrating bands correspond to the TetR'-Ssn6-5flag. Intensity of bands were
613 measured with ImageJ.
614
615 Figure S7 Regulation of *CDC5-5flag* expression by the iAID system
616 Cdc5 protein level expressed by the iAID system. Wild type diploid cells carrying either
617 P$_{TetO7}$-*CDC5-5flag* (HPH2049) or P$_{TetO7}$-*mAID-CDC5-5flag* (HPH2053) as well as P$_{ADH1}$-
618 *OsTIR*, P$_{CMV}$-tTA, P$_{OpTEF1}$-*TetR'-OpSSN6-5flag* and wild type diploid cells carrying P$_{ADH1}$-
619 *OsTIR* and P$_{OpTEF1}$-*TetR'-OpSSN6-5flag* were grown in SD medium supplemented with
620 appropriate nucleotide and amino acids in the presence of doxycycline at the indicated
621 concentation. IAA was added at 0.5 mM and incubated at 30 °C for 2.5 hrs. Total cell
622 extracts were prepared and subjected to a western analysis using anti-flag antibody. Intensity
623 of bands was quantified with ImageJ software.
624
625 Figure S8 Phenotype of the iAID-*hcd2-as* mutant

(A) Schematics of the plasmids used to construct the *iAID-hcd2-as* mutant carry in the hcd2 Δ background. The plasmids, pHM1153 and pHM1177, were integrated into *OpURA3* and *OpLEU1* loci, respectively. The maps were drawn with SnapGene.

(A) Growth assay of the iAID-*hcd2-as* mutant. Serial dilutions of strains with the indicated genotype were spotted on a YPDS agar plate and a YPDS plate containing 0.5 mM IAA, 20 μg/ml doxycycline, and 5μM NM-PP1 and incubated at 30 °C for 1day. Yeast strains: HPH2194, HPH2195, HPH2196, HPH2197, HPH2198.

(B) DAPI staining of iAID-*hcd2-as* strains. Wild type (HPH2176) and *iAID-hcd2-as* cells (HPH2105) carrying P_{ADH1}-*OsTIR*, P_{CMV}-tTA, P_{OpTEF1}-*TetR'-OpSSN6-5flag* as well as *hcd2-as* cells (HPH1870) were grown in YPDS medium until logarithmical growth phase. Doxycycline, IAA, and NM-PP1 were added at 5 μg/ml, 0.5 mM, and 5 μM, respectively, and incubated at 30 °C for 2 hrs. Cells were fixed with 70 % ethanol and DNA was stained with DAPI. Bright field image and DAPI image were merged. Scale bar, 10 μm. Arrows indicate failure of cell separation in the previous mitosis.

References

1. Baro B, Queralt E, Monje-Casas F. Regulation of Mitotic Exit in Saccharomyces cerevisiae. Methods Mol Biol 2017; 1505:3–17.

2. Meitinger F, Palani S, Pereira G. The power of MEN in cytokinesis. Cell Cycle 2012; 11:219–28.

3. Jaspersen SL, Charles JF, Tinker-Kulberg RL, Morgan DO. A late mitotic regulatory network controlling cyclin destruction in Saccharomyces cerevisiae. Mol Biol Cell 1998; 9:2803–17.

4. Luca FC, Winey M. MOB1, an essential yeast gene required for completion of mitosis and maintenance of ploidy. Mol Biol Cell 1998; 9:29–46.

5. Komarnitsky SI, Chiang YC, Luca FC, Chen J, Toyn JH, Winey M, Johnston LH, Denis CL. DBF2 protein kinase binds to and acts through the cell cycle-regulated MOB1 protein. Molecular and Cellular Biology 1998; 18:2100–7.

6. Guertin DA, Chang L, Irshad F, Gould KL, McCollum D. The role of the sid1p kinase and cdc14p in regulating the onset of cytokinesis in fission yeast. EMBO J 2000; 19:1803–15.

7. Kim J-M, Zeng CJT, Nayak T, Shao R, Huang A-C, Oakley BR, Liu B. Timely septation requires SNAD-dependent spindle pole body localization of the septation initiation network components in the filamentous fungus Aspergillus nidulans. Mol Biol Cell 2009; 20:2874–84.

8. Bates S. Candida albicans Cdc15 is essential for mitotic exit and cytokinesis. Sci Rep 2018; 8:8899.

9. Milne SW, Cheetham J, Lloyd D, Shaw S, Moore K, Paszkiewicz KH, Aves SJ, Bates S. Role of Candida albicans Tem1 in mitotic exit and cytokinesis. Fungal Genet Biol 2014; 69:84–95.

10. Saraya R, Krikken AM, Kiel JA, Baerends RJS, Veenhuis M, Klei IJ. Novel genetic tools for Hansenula polymorpha. FEMS Yeast Research 2012; 12:271–8.

11. Ito Y, Terai G, Ishigami M, Hashiba N, Nakamura Y, Bamba T, Kumokita R,

669 Hasunuma T, Asai K, Ishii J, et al. Exchange of endogenous and heterogeneous yeast
670 terminators in Pichia pastoris to tune mRNA stability and gene expression. Nucleic
671 Acids Res 2020; 48:13000–12.

672 12. Xiong X, Chen S. Expanding Toolbox for Genes Expression of Yarrowia lipolytica to
673 Include Novel Inducible, Repressible, and Hybrid Promoters. ACS Synth Biol 2020;
674 9:2208–13.

675 13. McIsaac RS, Oakes BL, Wang X, Dummit KA, Botstein D, Noyes MB. Synthetic gene
676 expression perturbation systems with rapid, tunable, single-gene specificity in yeast.
677 Nucleic Acids Res 2013; 41:e57–7.

678 14. Nishimura K, Fukagawa T, Takisawa H, Kakimoto T, Kanemaki M. An auxin-based
679 degron system for the rapid depletion of proteins in nonplant cells. Nat Methods 2009;
680 6:917–22.

681 15. Nishimura K, Kanemaki MT. Rapid depletion of budding yeast proteins via the fusion
682 of an auxin-inducible degron (AID). Current Protocols in Cell Biology 2014; 64:1–16.

683 16. Maekawa H, Neuner A, Rüthnick D, Schiebel E, Pereira G, Kaneko Y. Polo-like
684 kinase Cdc5 regulates Spc72 recruitment to spindle pole body in the methylotrophic
685 yeast Ogataea polymorpha. eLife 2017; 6:e24340.

686 17. Nishimura K, Yamada R, Hagihara S, Iwasaki R, Uchida N, Kamura T, Takahashi K,
687 Torii KU, Fukagawa T. A super-sensitive auxin-inducible degron system with an
688 engineered auxin-TIR1 pair. Nucleic Acids Res 2020; 48:e108.

689 18. Tanaka S, Miyazawa-Onami M, Iida T, Araki H. iAID: an improved auxin-inducible
690 degron system for the construction of a “tight” conditional mutant in the budding yeast
691 Saccharomyces cerevisiae. Yeast 2015; 32:567–81.

692 19. Lu SF, Tolstorukov II, Anamnart S, Kaneko Y, Harashima S. Cloning, sequencing,
693 and functional analysis of H-OLE1 gene encoding delta9-fatty acid desaturase in
694 Hansenula polymorpha. Appl Microbiol Biotechnol 2000; 54:499–509.

695 20. Janke C, Magiera MM, Rathfelder N, Taxis C, Reber S, Maekawa H, Moreno-
696 Borchart A, Doenges G, Schwob E, Schiebel E, et al. A versatile toolbox for PCR-

based tagging of yeast genes: new fluorescent proteins, more markers and promoter substitution cassettes. Yeast 2004; 21:947–62.

21. Faber KN, Haima P, Harder W, Veenhuis M, AB G. Highly-efficient electrotransformation of the yeast Hansenula polymorpha. Current Genetics 1994; 25:305–10.

22. Bellí G, Garí E, Aldea M, Herrero E. Functional analysis of yeast essential genes using a promoter-substitution cassette and the tetracycline-regulatable dual expression system. Yeast 1998; 14:1127–38.

23. Sherman F. Getting started with yeast. Meth Enzymol 1991; 194:3–21.

24. Chen H, Clyborne WK, Sedat JW, Agard DA. PRIISM: an integrated system for display and analysis of 3-D microscope images. SPIE/IS&T 1992 Symposium on Electronic Imaging: Science and Technology 1992; 1660:784–90.

25. Maekawa H, Kaneko Y. Inversion of the chromosomal region between two mating type loci switches the mating type in Hansenula polymorpha. PLoS Genet 2014; 10:e1004796.

26. Knop M, Siegers K, Pereira G, Zachariae W, Winsor B, Nasmyth K, Schiebel E. Epitope tagging of yeast genes using a PCR-based strategy: More tags and improved practical routines. Yeast 1999; 15:963–72.

27. Meitinger F, Palani S, Pereira G. Detection of Phosphorylation Status of Cytokinetic Components. Methods Mol Biol 2016; 1369:219–37.

28. Bishop AC, Ubersax JA, Petsch DT, Matheos DP, Gray NS, Blethrow J, Shimizu E, Tsien JZ, Schultz PG, Rose MD, et al. A chemical switch for inhibitor-sensitive alleles of any protein kinase. Nature 2000; 407:395–401.

29. D'Aquino KE, Monje-Casas F, Paulson J, Reiser V, Charles GM, Lai L, Shokat KM, Amon A. The protein kinase Kin4 inhibits exit from mitosis in response to spindle position defects. Molecular Cell 2005; 19:223–34.

30. Bellí G, Garí E, Piedrafita L, Aldea M, Herrero E. An activator/repressor dual system allows tight tetracycline-regulated gene expression in budding yeast. Nucleic Acids

Res 1998; 26:942–7.

31. Yesbolatova A, Saito Y, Kitamoto N, Makino-Itou H, Ajima R, Nakano R, Nakaoka H, Fukui K, Gamo K, Tominari Y, et al. The auxin-inducible degron 2 technology provides sharp degradation control in yeast, mammalian cells, and mice. Nature Communications 2020; 11:5701–13.

32. Rock JM, Amon A. Cdc15 integrates Tem1 GTPase-mediated spatial signals with Polo kinase-mediated temporal cues to activate mitotic exit. Genes & Development 2011; 25:1943–54.

33. Shen X-X, Zhou X, Kominek J, Kurtzman CP, Hittinger CT, Rokas A. Reconstructing the Backbone of the Saccharomycotina Yeast Phylogeny Using Genome-Scale Data. G3 (Bethesda) 2016; 6:3927–39.

34. Nordberg H, Cantor M, Dusheyko S, Hua S, Poliakov A, Shabalov I, Smirnova T, Grigoriev IV, Dubchak I. The genome portal of the Department of Energy Joint Genome Institute: 2014 updates. Nucleic Acids Res 2014; 42:D26–31.

35. Waterhouse AM, Procter JB, Martin DMA, Clamp M, Barton GJ. Jalview Version 2-a multiple sequence alignment editor and analysis workbench. Bioinformatics 2009; 25:1189–91.

Figure 1

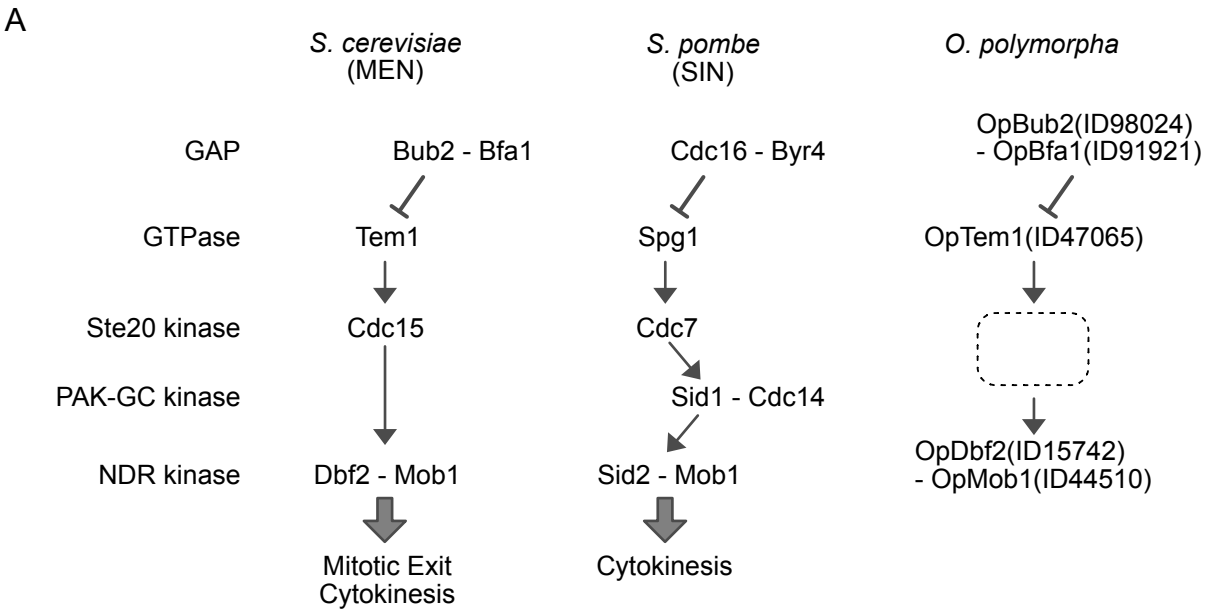

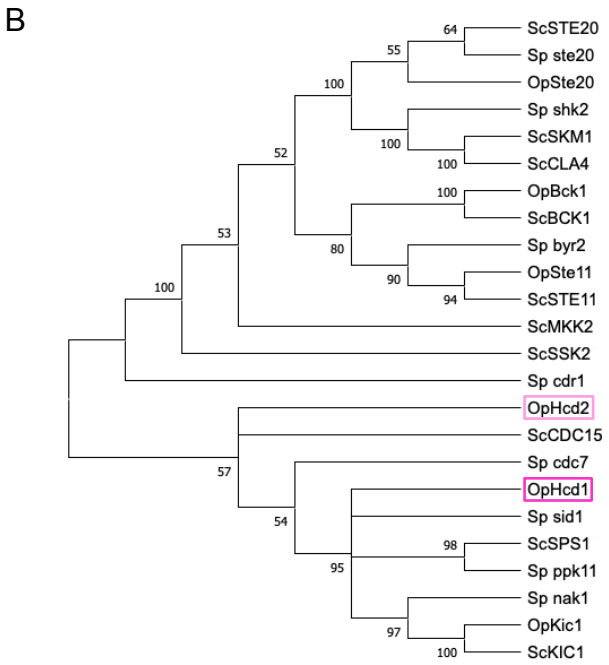

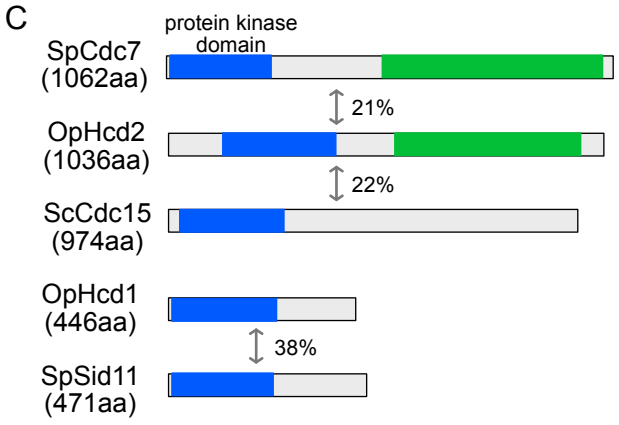

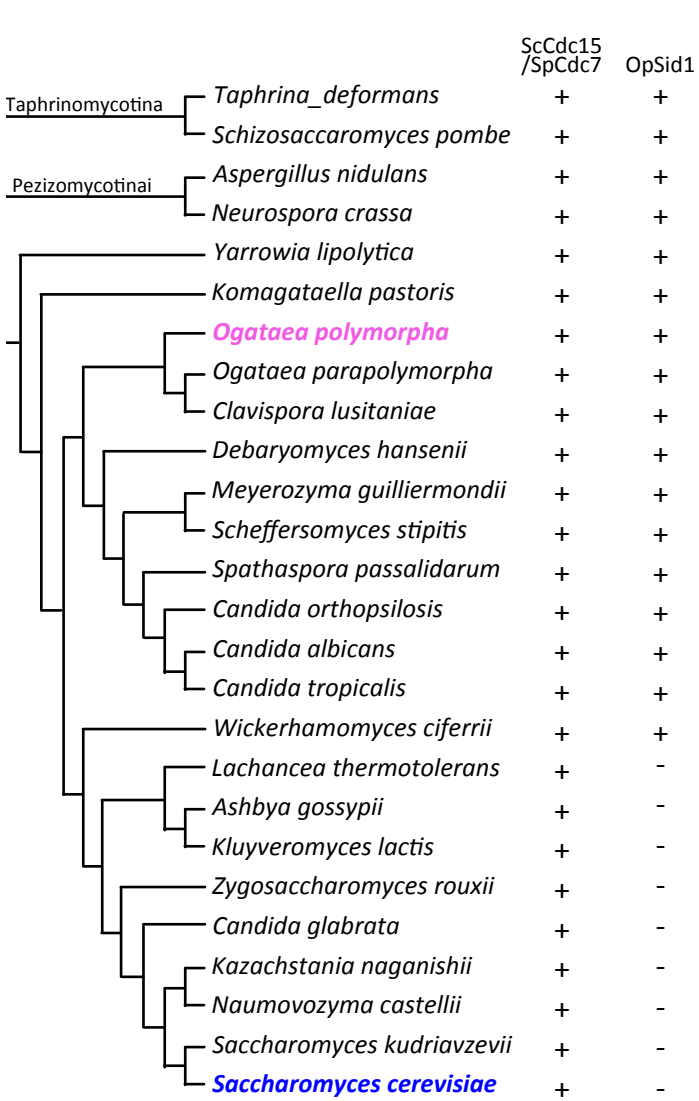

Figure 2

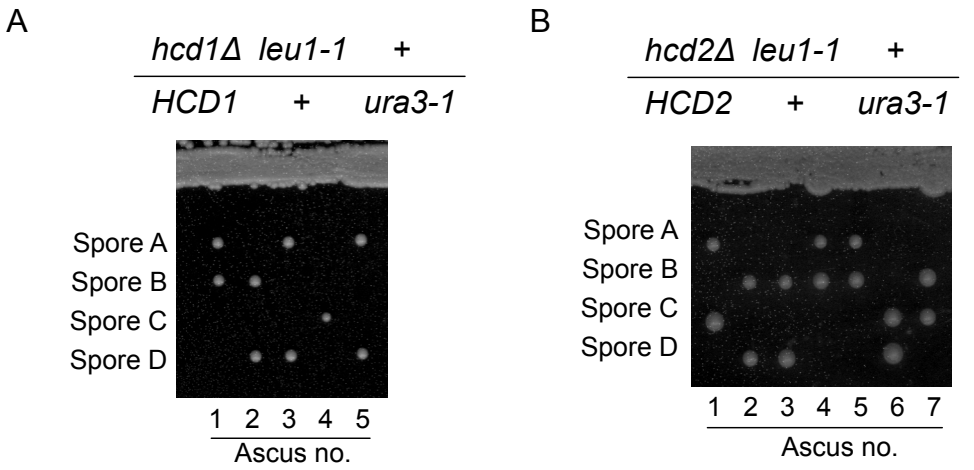

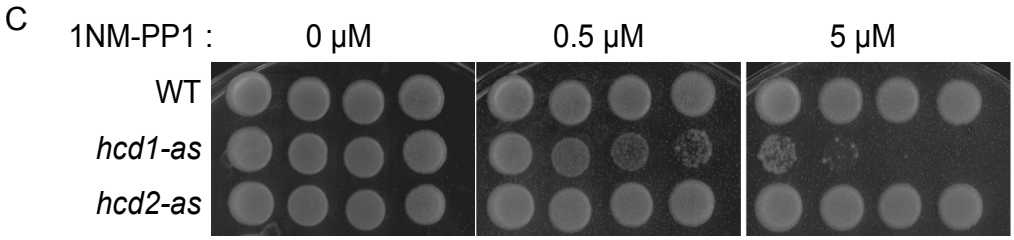

Figure 3

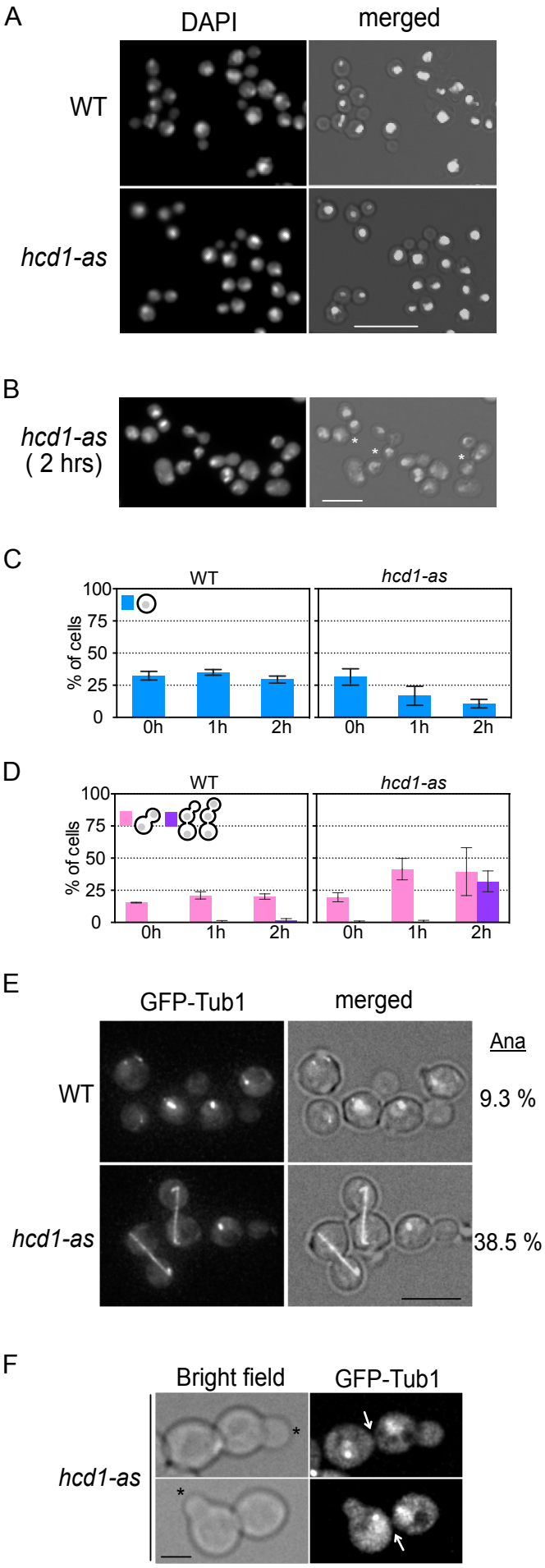

Figure 4

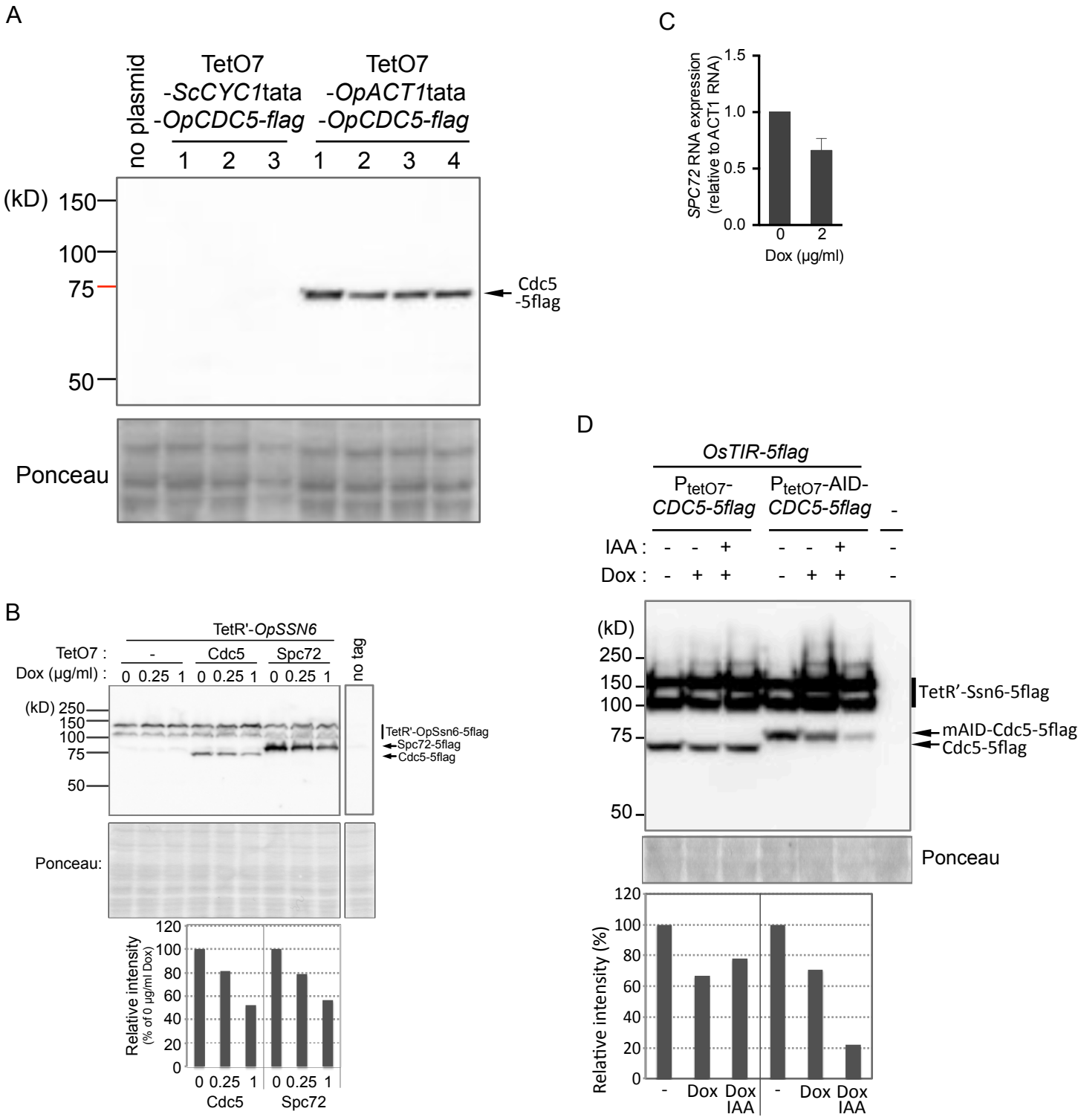

Figure 5